First measurement of coherent ϕ-meson photoproduction on deuteron at low energies

T. Mibe,[1] H. Gao,[2] K. Hicks,[1] K. Kramer,[2] S. Stepanyan,[3] D.J. Tedeschi,[4] M.J. Amaryan,[31] P. Ambrozewicz,[16] M. Anghinolfi,[22] G. Asryan,[39] G. Audit,[11] H. Avakian,[3] H. Bagdasaryan,[31] N. Baillie,[38] J.P. Ball,[6] N.A. Baltzell,[4] M. Battaglieri,[22] I. Bedlinskiy,[24] M. Bellis,[9] N. Benmouna,[18] B.L. Berman,[18] A.S. Biselli,[9, 15] L. Blaszczyk,[17] S. Bouchigny,[23] S. Boiarinov,[3] R. Bradford,[9] D. Branford,[14] W.J. Briscoe,[18] W.K. Brooks,[3] S. Bültmann,[31] V.D. Burkert,[3] C. Butuceanu,[38] J.R. Calarco,[29] S.L. Careccia,[31] D.S. Carman,[3] S. Chen,[17] P.L. Cole,[10, 20, 3] P. Collins,[6] P. Coltharp,[17] D. Crabb,[37] H. Crannell,[10] V. Crede,[17] J.P. Cummings,[32] N. Dashyan,[39] R. De Masi,[11] R. De Vita,[22] E. De Sanctis,[21] P.V. Degtyarenko,[3] A. Deur,[3] K.V. Dharmawardane,[31] R. Dickson,[9] C. Djalali,[4] G.E. Dodge,[31] J. Donnelly,[19] D. Doughty,[12, 3] M. Dugger,[6] O.P. Dzyubak,[4] H. Egiyan,[3, *] K.S. Egiyan,[39] L. El Fassi,[5] L. Elouadrhiri,[3] P. Eugenio,[17] G. Fedotov,[28] G. Feldman,[18] H. Funsten,[38] M. Garçon,[11] G. Gavalian,[29, 31] G.P. Gilfoyle,[34] K.L. Giovanetti,[25] F.X. Girod,[11, 3] J.T. Goetz,[7] A. Gonenc,[16] C.I.O. Gordon,[19] R.W. Gothe,[4] K.A. Griffioen,[38] M. Guidal,[23] N. Guler,[31] L. Guo,[3] V. Gyurjyan,[3] C. Hadjidakis,[23] K. Hafidi,[5] H. Hakobyan,[39] R.S. Hakobyan,[10] C. Hanretty,[17] J. Hardie,[12, 3] F.W. Hersman,[29] I. Hleiqawi,[1] M. Holtrop,[29] C.E. Hyde-Wright,[31] Y. Ilieva,[18] D.G. Ireland,[19] B.S. Ishkhanov,[28] E.L. Isupov,[28] M.M. Ito,[3] D. Jenkins,[36] H.S. Jo,[23] J.R. Johnstone,[19] K. Joo,[13] H.G. Juengst,[18, 31] N. Kalantarians,[31] J.D. Kellie,[19] M. Khandaker,[30] W. Kim,[26] A. Klein,[31] F.J. Klein,[10] A.V. Klimenko,[31] M. Kossov,[24] Z. Krahn,[9] L.H. Kramer,[16, 3] V. Kubarovsky,[32] J. Kuhn,[9] S.E. Kuhn,[31] S.V. Kuleshov,[24] V.Kuznetsov,[26] J. Lachniet,[9, 31] J.M. Laget,[11, 3] J. Langheinrich,[4] D. Lawrence,[27] T. Lee,[29] Ji Li,[32] K. Livingston,[19] H.Y. Lu,[4] M. MacCormick,[23] C. Marchand,[11] N. Markov,[13] P. Mattione,[33] B. McKinnon,[19] B.A. Mecking,[3] J.J. Melone,[19] M.D. Mestayer,[3] C.A. Meyer,[9] K. Mikhailov,[24] R. Minehart,[37] M. Mirazita,[21] R. Miskimen,[27] V. Mokeev,[28] K. Moriya,[9] S.A. Morrow,[23, 11] M. Moteabbed,[16] E. Munevar,[18] G.S. Mutchler,[33] P. Nadel-Turonski,[18] R. Nasseripour,[16, 4] S. Niccolai,[23] G. Niculescu,[25] I. Niculescu,[25] B.B. Niczyporuk,[3] M.R. Niroula,[31] R.A. Niyazov,[3] M. Nozar,[3, †] M. Osipenko,[22, 28] A.I. Ostrovidov,[17] K. Park,[26] E. Pasyuk,[6] C. Paterson,[19] S. Anefalos Pereira,[21] J. Pierce,[37] N. Pivnyuk,[24] D. Pocanic,[37] O. Pogorelko,[24] S. Pozdniakov,[24] J.W. Price,[8] Y. Prok,[37, 3, ‡] D. Protopopescu,[19] B.A. Raue,[16, 3] G. Riccardi,[17] G. Ricco,[22] M. Ripani,[22] B.G. Ritchie,[6] F. Ronchetti,[21] G. Rosner,[19] P. Rossi,[21] F. Sabatié,[11] J. Salamanca,[20] C. Salgado,[30] J.P. Santoro,[36, 3, §] V. Sapunenko,[3] R.A. Schumacher,[9] V.S. Serov,[24] Y.G. Sharabian,[3] D. Sharov,[28] N.V. Shvedunov,[28] E.S. Smith,[3] L.C. Smith,[37] D.I. Sober,[10] D. Sokhan,[14] A. Stavinsky,[24] S.S. Stepanyan,[26] B.E. Stokes,[17] P. Stoler,[32] I.I. Strakovsky,[18] S. Strauch,[18, 4] M. Taiuti,[22] U. Thoma,[3, ¶] A. Tkabladze,[1, 18] S. Tkachenko,[31] L. Todor,[34] C. Tur,[4] M. Ungaro,[32, 13] M.F. Vineyard,[35] A.V. Vlassov,[24] D.P. Watts,[19, **] L.B. Weinstein,[31] D.P. Weygand,[3] M. Williams,[9] E. Wolin,[3] M.H. Wood,[4, ††] A. Yegneswaran,[3] L. Zana,[29] J. Zhang,[31] B. Zhao,[13] and Z.W. Zhao[4]

(The CLAS Collaboration)

[1]*Ohio University, Athens, Ohio 45701*
[2]*Duke University, Durham, North Carolina 27708*
[3]*Thomas Jefferson National Accelerator Facility, Newport News, Virginia 23606*
[4]*University of South Carolina, Columbia, South Carolina 29208*
[5]*Argonne National Laboratory, Argonne, IL 60439*
[6]*Arizona State University, Tempe, Arizona 85287-1504*
[7]*University of California at Los Angeles, Los Angeles, California 90095-1547*
[8]*California State University, Dominguez Hills, Carson, CA 90747*
[9]*Carnegie Mellon University, Pittsburgh, Pennsylvania 15213*
[10]*Catholic University of America, Washington, D.C. 20064*
[11]*CEA-Saclay, Service de Physique Nucléaire, 91191 Gif-sur-Yvette, France*
[12]*Christopher Newport University, Newport News, Virginia 23606*
[13]*University of Connecticut, Storrs, Connecticut 06269*
[14]*Edinburgh University, Edinburgh EH9 3JZ, United Kingdom*
[15]*Fairfield University, Fairfield CT 06824*
[16]*Florida International University, Miami, Florida 33199*
[17]*Florida State University, Tallahassee, Florida 32306*
[18]*The George Washington University, Washington, DC 20052*
[19]*University of Glasgow, Glasgow G12 8QQ, United Kingdom*
[20]*Idaho State University, Pocatello, Idaho 83209*
[21]*INFN, Laboratori Nazionali di Frascati, 00044 Frascati, Italy*
[22]*INFN, Sezione di Genova, 16146 Genova, Italy*
[23]*Institut de Physique Nucleaire ORSAY, Orsay, France*
[24]*Institute of Theoretical and Experimental Physics, Moscow, 117259, Russia*

^{25}*James Madison University, Harrisonburg, Virginia 22807*
^{26}*Kyungpook National University, Daegu 702-701, Republic of Korea*
^{27}*University of Massachusetts, Amherst, Massachusetts 01003*
^{28}*Moscow State University, General Nuclear Physics Institute, 119899 Moscow, Russia*
^{29}*University of New Hampshire, Durham, New Hampshire 03824-3568*
^{30}*Norfolk State University, Norfolk, Virginia 23504*
^{31}*Old Dominion University, Norfolk, Virginia 23529*
^{32}*Rensselaer Polytechnic Institute, Troy, New York 12180-3590*
^{33}*Rice University, Houston, Texas 77005-1892*
^{34}*University of Richmond, Richmond, Virginia 23173*
^{35}*Union College, Schenectady, NY 12308*
^{36}*Virginia Polytechnic Institute and State University, Blacksburg, Virginia 24061-0435*
^{37}*University of Virginia, Charlottesville, Virginia 22901*
^{38}*College of William and Mary, Williamsburg, Virginia 23187-8795*
^{39}*Yerevan Physics Institute, 375036 Yerevan, Armenia*
(Dated: February 8, 2008)

The cross section and decay angular distributions for the coherent ϕ meson photoproduction on the deuteron have been measured for the first time up to a squared four-momentum transfer $t = (p_\gamma - p_\phi)^2 = -2 \text{ GeV}^2/\text{c}^2$, using the CLAS detector at the Thomas Jefferson National Accelerator Facility. The cross sections are compared with predictions from a re-scattering model. In a framework of vector meson dominance, the data are consistent with the total ϕ-N cross section $\sigma_{\phi N}$ at about 10 mb. If vector meson dominance is violated, a larger $\sigma_{\phi N}$ is possible by introducing larger t-slope for the $\phi N \to \phi N$ process than that for the $\gamma N \to \phi N$ process. The decay angular distributions of the ϕ are consistent with helicity conservation.

The exchange of gluons between hadrons, known as Pomeron exchange [1], is a fundamental process that is expected to dominate hadron-hadron total cross sections at high energies. In general, multi-gluon exchange is harder to study at lower energy since diagrams including quark exchange play a more important role. The ϕ meson is unique in that it is nearly pure $s\bar{s}$ and hence multi-gluon exchange is expected to dominate ϕ-N scattering at all energies. Since gluon exchange is flavor blind, information on multi-gluon exchange, isolated from the ϕ-N interaction, would be universal and useful in models of hadron-hadron interactions. For example, information on the ϕ-N interaction at very low energies, known as the QCD van der Waals interaction, is essential for the reliable prediction of the possible formation of a bound state in the ϕ-N system [2].

The total ϕ-N cross section ($\sigma_{\phi N}$) is estimated by using vector meson dominance (VMD) applied to exclusive ϕ photoproduction on the proton in the photon energy range $E_\gamma < 10$ GeV, resulting in $\sigma_{\phi N} \simeq 10$–12 mb [3, 4], which is in agreement with the estimate from the additive quark model [5] applied to KN and πN scattering data [6]. More recently, the inelastic ϕ-N cross section $\sigma_{\phi N}^{inel}$ was extracted from the attenuation of ϕ-mesons in photoproduction from Li, C, Al, and Cu nuclei [7]. The attenuation for large A is significantly larger than that calculated from VMD. More sophisticated models [4, 8, 9] are consistent with the experiment if $\sigma_{\phi N}^{inel}$ is significantly larger ($\sim$30 mb) compared with $\sigma_{\phi N}$ from the VMD model. The reason for the discrepancy of $\sigma_{\phi N}$ from these two estimates is not well understood. Here we will show that information on the t dependence and spin structure of the ϕ-N interaction provides essential clues to solve this problem.

In this Letter, the ϕ-N interaction is investigated in coherent photoproduction on deuterium. The diagrams of the dominant processes contributing to the reaction $\gamma d \to \phi d$ are shown in Fig. 1. In the first diagram, Fig. 1(a), the ϕ is produced in a single scattering of a nucleon, which is dominant at small $-t$, and strongly suppressed at larger $-t$ due to the deuteron form factor. The second diagram, Fig. 1(b), shows double-scattering, where the ϕ is produced at the first vertex and scatters from the other nucleon at the second vertex. The strength of the second interaction is gauged by $\sigma_{\phi N}$. The probability to undergo double-scattering increases at larger $-t$ because both nucleons receive momentum transfer and may recombine into a final-state deuteron with a smaller relative momentum between the two nucleons [10].

The ϕ meson is a spin one particle which decays to a $K\bar{K}$ pair, *i.e.* two spin-less particles. The decay angular distribution of the ϕ carries information on the spin structure of the reaction amplitude which is the sum of single- and double- scattering processes [11].

The measurement of the differential cross sections of coherent ϕ photoproduction and the decay angular distributions in a wide t range allows one to study the ϕ-N interaction in both single and double scattering, as well as the transition from one to the other.

The data were collected with the CLAS detector and the Hall B tagged-photon beam at the Thomas Jefferson
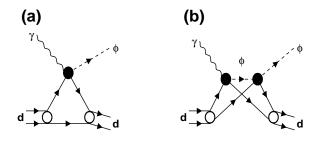
FIG. 1: (a) Single-scattering and (b) double-scattering contributions to the coherent ϕ-meson photoproduction on the deuteron.

FIG. 2: (a) Missing mass distribution of the reaction $\gamma d \rightarrow d K^+ X$ for events near the ϕ-meson mass ($0.98 < M(K^+K^-) < 1.12$ GeV/c^2). (b) Invariant mass distribution for the K^+K^- pair after the selection of the missing K^-. The solid curve is a fit to the data. The dashed curve shows the contribution from background.

National Accelerator Facility [12]. The incident electron beam energy was 3.8 GeV, producing tagged photons in the range from 0.8 to 3.6 GeV. The photon beam was directed onto a 24-cm long liquid-deuterium target. The data acquisition trigger required two charged particles detected in coincidence with a tagged photon. Charged particles were momentum analyzed by the CLAS torus magnet and three sets of drift chambers. The torus magnet was run at two settings, low field (2250 A) and high field (3375 A), each for about half of the run period.

The reaction $\gamma d \rightarrow \phi d$ was identified by detecting a deuteron and a K^+ from $\phi \rightarrow K^+K^-$ decay. The K^+ and deuteron were selected based on time-of-flight, path length, and momentum measurements. Figure 2(a) shows the missing mass distribution, M_X, for the reaction $\gamma d \rightarrow d K^+ X$ when events near the ϕ-meson peak ($0.98 < M(K^+K^-) < 1.12$ GeV/c^2) were selected in the K^+K^- invariant mass, assuming a K^- was the missing particle. A missing K^- peak is seen on top of a smooth background from non-d K^+K^- final states. The missing mass resolution, ranging from 8 to 30 MeV/c^2, depends on photon energy and the deuteron momentum. A three-σ cut was applied to select the missing K^- for the exclusive $\gamma d \rightarrow K^+K^-d$ reaction.

Figure 2(b) shows the invariant mass distribution for the K^+K^- pair after the selection of the missing K^-. The ϕ-meson peak appears above a smooth background. The ϕ-meson yield was obtained from a fit to the $M(K^+K^-)$ distribution by a gaussian-convoluted Breit-Wigner function and a background function. The width and the pole position for the Breit-Wigner function were fixed to 4.3 MeV/c^2 and 1019.5 MeV/c^2, respectively [13]. The standard deviation of the gaussian distribution was fixed to the value obtained from simulation. The background function was chosen as $a\sqrt{x^2 - (2m_K)^2} + b(x^2 - (2m_K)^2)$ [14], where x is $M(K^+K^-)$, m_K is the charged kaon mass, and a and b are the fit parameters. Three background functions: a linear background, background from non-resonan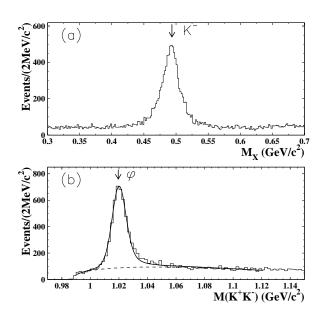t K^+K^-d production, and f_0 photoproduction, were studied as alternative choices. The background models for the non-resonant K^+K^-d and f_0 photoproduction were parameterized by the differential cross section and photon-energy distribution of events in the sidebands of the ϕ-meson peak. The dependence of the yield on the background function, fit range, and parameterization of the Breit-Wigner function were studied. The extracted yield changes between 3% and 9% depending on the yield extraction procedures.

The CLAS acceptance was determined by using a GEANT-based Monte Carlo simulation [15]. The simulation was iterated to reproduce measured t, photon energy, and decay angular distributions. The acceptance was between 10% and 20% in the kinematic region covered by the present measurements. The accuracy of the calculation of the acceptance was estimated from comparison of results from the other event reconstruction topologies (d K^+K^-, K^+K^-, and d K_s^0 topologies) for which the acceptances were different from that for the d K^+ topology. The differential cross sections for these topologies are shown in Fig. 3. They agree with each other within statistical uncertainties, indicating that the acceptance is understood as to the number of reconstructed tracks, charge combinations, and decay modes. Supplemental simulations were performed to understand the systematic uncertainties due to the event generator (1-11%) and event reconstruction (1-5%).
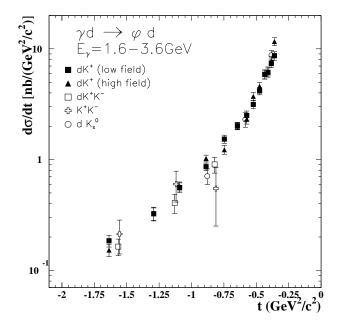
FIG. 3: Comparison of differential cross sections for $\gamma d \to \phi d$ from various topologies in the range $1.6 < E_\gamma < 3.6$ GeV. Only statistical uncertainties are shown.

TABLE I: Differential cross sections for the reaction $\gamma d \to \phi d$. The second and third numbers in each field are the statistical and systematic uncertainties, respectively.

t range (GeV^2/c^2)		$d\sigma/dt$ $[\text{nb}/(\text{GeV}^2/c^2)]$	
t_{min}	t_{max}	$1.6 < E_\gamma < 2.6$ GeV	$2.6 < E_\gamma < 3.6$ GeV
-0.375	-0.350	$10.21 \pm 0.82\ (1.70)$	$8.63 \pm 0.80\ (1.04)$
-0.400	-0.375	$8.85 \pm 0.75\ (1.11)$	$6.80 \pm 0.69\ (1.07)$
-0.425	-0.400	$7.32 \pm 0.59\ (0.94)$	$4.57 \pm 0.53\ (0.74)$
-0.450	-0.425	$6.16 \pm 0.55\ (0.81)$	$5.76 \pm 0.56\ (0.65)$
-0.500	-0.450	$4.73 \pm 0.34\ (0.60)$	$3.99 \pm 0.33\ (0.55)$
-0.550	-0.500	$3.52 \pm 0.28\ (0.51)$	$3.59 \pm 0.29\ (0.55)$
-0.600	-0.550	$2.66 \pm 0.24\ (0.38)$	$2.11 \pm 0.22\ (0.28)$
-0.700	-0.600	$2.17 \pm 0.15\ (0.26)$	$1.83 \pm 0.14\ (0.24)$
-0.800	-0.700	$1.40 \pm 0.12\ (0.16)$	$1.32 \pm 0.12\ (0.20)$
-1.000	-0.800	$0.94 \pm 0.07\ (0.11)$	$0.96 \pm 0.07\ (0.11)$
-1.200	-1.000	$0.57 \pm 0.06\ (0.07)$	$0.57 \pm 0.05\ (0.06)$
-1.400	-1.200	$0.28 \pm 0.05\ (0.04)$	$0.36 \pm 0.04\ (0.05)$
-2.000	-1.400	$0.19 \pm 0.02\ (0.03)$	$0.15 \pm 0.02\ (0.02)$

Systematic uncertainties in the yield extraction and acceptance were estimated as a function of photon energy and t; they were between 4% and 13%. The combined systematic uncertainty for the luminosity and trigger efficiency was less than 10%. Systematic uncertainties from contributions from accidental tracks, target windows, and particle misidentification are less than a few percent. The total systematic uncertainty was estimated as 11-17% by adding these uncertainties in quadrature.

The differential cross sections were measured in the ranges $1.6 < E_\gamma < 2.6$ GeV and $2.6 < E_\gamma < 3.6$ GeV. They are given in Table I. Figure 4 shows the experimental data in the range $2.6 < E_\gamma < 3.6$ GeV. The data is compared with theoretical calculations using a rescattering model [10, 16]. In this model, the $\gamma N \to \phi N$ amplitude was parameterized by using published data on the $\gamma p \to \phi p$ reaction [17] and data from the proton target run during this experiment. This amplitude was convoluted with the deuteron wave function with a correction of the relativistic-recoil effect [10]. The double scattering process (Fig. 1(b)) is modeled by the Generalized Eikonal Approximation [18]. The $\sigma_{\phi N}$ and t dependence for the re-scattering process are the inputs for the calculation. The model successfully reproduces the differential cross sections on coherent ρ photoproduction [10] using the inputs from the VMD.

The total model uncertainty is estimated to be about 20%. A 10% uncertainty was assigned to the parametrization of the $\gamma N \to \phi N$ amplitude based on

the $\gamma p \to \phi p$ data. The effect of spin-flip in the process $\gamma N \to \phi N$ was ignored in the parametrization of the single scattering amplitude since the spin-flip amplitude is more suppressed in the coherent process than in the incoherent process. A 15% systematic uncertainty was assigned due to this effect [19]. An isospin dependence of the process $\gamma N \to \phi N$ was not taken into account in the model, but Ref. [20] suggests such an effect is small.

In Fig. 4, curve A shows the t distribution calculated by using the VMD prediction for the ϕ-N cross section, i.e. $\sigma_{\phi N}$=10 mb, and the same t distribution for the reaction $\gamma N \to \phi N$ and the reaction $\phi N \to \phi N$. The curve B corresponds to $\sigma_{\phi N}$=30 mb, inspired by Ref. [7], with the VMD assumption for the t distribution. It overestimates the data at large $-t$ where the contribution from double scattering dominates. This implies that if the t distribution follows the VMD prediction, $\sigma_{\phi N}$ should also be consistent with the VMD prediction. In this case, inconsistency with the larger $\sigma_{\phi N}$ from the A-dependence experiment [7] still remains.

However, the VMD picture may not be a good approximation in this photon energy range. The larger $\sigma_{\phi N}$ from the A-dependence experiment [7] can be explained if the t distribution of the reaction $\phi N \to \phi N$ is different from the VMD prediction. For example, it is possible for the virtual ϕ to fluctuate to a $K\bar{K}$ pair and have a larger cross section for the second interaction [21]. In this case, the t-slope for the second interaction would be larger than that for the $\gamma N \to \phi N$ reaction based on a general geometric relation between the t-slope and the total cross section [22]. Following this hypothesis, cross sections were calculated with $\sigma_{\phi N}$=30 mb using a larger
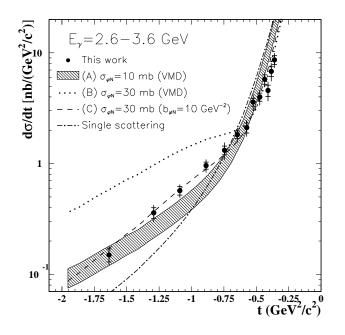
FIG. 4: Differential cross sections for the reaction $\gamma d \to \phi d$. The inner error bars shown are statistical uncertainty only, while the outer error bars are the sum of statistical and systematic uncertainties in quadrature. The curves A, B and C are calculations from the re-scattering model [10, 16], see text for details. The uncertainties on curves B and C are comparable to that of curve A, but are not shown. The dot-dashed curve is a contribution from the single scattering diagram.

exponential t-slope, $b_{\phi N} = 10$ (GeV/c)$^{-2}$, in the second interaction (curve C). The data is equally-well described by curve C, suggesting a larger t-slope parameter is necessary if $\sigma_{\phi N}$ is larger than the VMD prediction. Although the current data do not allow one to extract the $\sigma_{\phi N}$ and the t-slope independently due to the strong correlation between them, it possibly suggests a larger $\sigma_{\phi N}$ from the A-dependence.

In addition to the differential cross sections, the decay angular distributions of the ϕ meson were also measured in the helicity frame [11]. The direction of the ϕ-meson momentum in the CM system was chosen as the z-axis, and the polar angle and azimuthal angle between the K^+ momentum and the ϕ-meson production plane were defined as θ_H and ϕ_H in the ϕ-meson rest frame. Figure 5 shows the projections of the decay angular distributions onto $\cos\theta_H$ and ϕ_H in the ranges $-0.8 < t < -0.35$ GeV^2/c^2 and $-2.0 < t < -0.8$ GeV^2/c^2 in each photon energy region. The data are consistent with the prediction from helicity conservation (solid curves), *i.e.* the spin of the ϕ-meson is aligned to the momentum of the ϕ-meson. This is similar to what was observed in the ϕ photoproduction on the proton [23, 24]. In the larger $-t$ region, the double scattering contribution becomes more important. No drastic change is observed from the

smaller $-t$ to the larger $-t$ region, implying that the spin structure of the single- and double-scattering processes are similar.

In summary, we have presented the first measurement of the differential cross sections and decay angular distributions for coherent ϕ photoproduction on the deuteron up to $t = -2.0$ GeV^2/c^2. The differential cross sections at large $-t$ exhibit a contribution from double scattering. The data are consistent with $\sigma_{\phi N}=10$ mb in a framework of VMD. The data also provide a possible explanation for larger $\sigma_{\phi N}$ if the t-slope for $\phi N \to \phi N$ is larger than the VMD value from $\gamma p \to \phi p$. The decay angular distributions follow the prediction from helicity conservation.

This measurement demonstrates a new approach to the study of the ϕ-N interaction in the low energy region where VMD is not necessarily a good approximation. Further measurements at higher photon energies [25], at very small $-t$ [26], as well as an A-dependence study in e^+e^- decay [27] will make it possible to map out details of the energy and t dependences of the ϕ-N interaction.

* Current address:University of New Hampshire, Durham, New Hampshire 03824-3568
† Current address:TRIUMF, 4004, Wesbrook Mall, Vancouver, BC, V6T 2A3, Canada
‡ Current address:Massachusetts Institute of Technology, Cambridge, Massachusetts 02139-4307
§ Current address:Catholic University of America, Washington, D.C. 20064
¶ Current address:Physikalisches Institut der Universitaet Giessen, 35392 Giessen, Germany
** Current address:Edinburgh University, Edinburgh EH9 3JZ, United Kingdom
†† Current address:University of Massachusetts, Amherst, Massachusetts 01003

[1] A. Donnachie, H. G. Dosch, P. V. Landshoff, and O. Nachtmann, *Pomeron Physics and QCD* (Cambridge University Press, 2002).
[2] H. Gao, T. S. H. Lee, and V. Marinov, Phys. Rev. **C63**, 022201(R) (2001).
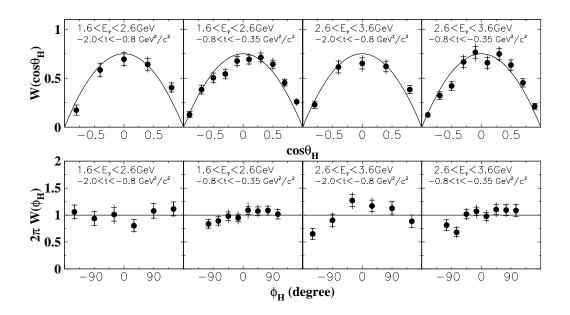[3] H. J. Behrend et al., Nucl. Phys. **B144**, 22 (1978).

FIG. 5: Decay angular distributions of the ϕ-meson in the helicity frame. The inner error bars shown are statistical uncertainty only, while the outer error bars are the sum of statistical and systematic uncertainties in quadrature. Solid curves are the predictions from helicity conservation.

[4] A. Sibirtsev, H. W. Hammer, U. G. Meissner, and A. W. Thomas, Eur. Phys. J. **A 29**, 209 (2006).
[5] H. J. Lipkin, Phys. Rev. Lett. **16**, 1015 (1966).
[6] A. H. Rosenfeld and P. Söding, *Properties of the Fundamental Interactions* (Editrice Compositori, Bologna, 1973), vol. 9, p. 882.
[7] T. Ishikawa et al., Phys. Lett. **B608**, 215 (2005).
[8] D. Cabrera, L. Roca, E. Oset, H. Toki, and M. J. Vicente Vacas, Nucl. Phys. **A733**, 130 (2004).
[9] P. Muhlich and U. Mosel, Nucl. Phys. **A765**, 188 (2006).
[10] L. Frankfurt et al., Nucl. Phys. **A622**, 511 (1997).
[11] K. Schilling, P. Seyboth, and G. E. Wolf, Nucl. Phys. **B15**, 397 (1970).
[12] B. A. Mecking et al., Nucl. Instrum. Meth. **A503**, 513 (2003).
[13] W. M. Yao et al. (Particle Data Group), J. Phys. **G33**, 1 (2006).
[14] K. Lukashin et al., Phys. Rev. **C63**, 065205 (2001).
[15] R. Brun, R. Hagelberg, M. Hansroul, and J. C. Lassalle (1978), CERN-DD-78-2-REV.
[16] T. C. Rogers, M. M. Sargsian, and M. I. Strikman, Phys. Rev. **C73**, 045202 (2006).
[17] E. Anciant et al., Phys. Rev. Lett. **85**, 4682 (2000).
[18] L. L. Frankfurt, M. M. Sargsian, and M. I. Strikman, Phys. Rev. **C56**, 1124 (1997).
[19] A. I. Titov, private communications.
[20] A. I. Titov, T. S. H. Lee, and H. Toki, Phys. Rev. **C59**, R2993 (1999).
[21] T. C. Rogers, M. M. Sargsian, and M. Strikman, private communications.
[22] B. Povh and J. Hufner, Phys. Rev. Lett. **58**, 1612 (1987).
[23] K. McCormick et al., Phys. Rev. **C69**, 032203 (2004).
[24] T. Mibe et al., Phys. Rev. Lett. **95**, 182001 (2005).
[25] R. Gothe, M. Holtrop, E. Smith, S. Stepanyan, et al., Jefferson Laboratory experiment E04-010, PAC25 proposal.
[26] W. C. Chang et al., private communications.
[27] M. H. Wood et al. (2006), CLAS Approved Analysis proposal.